

Covering Pressure and Friction Effect on Bending Stiffness and Natural Frequency for Braid-coated Biconvex Tape Boom

By Nobuhisa KATSUMATA,¹⁾ Ryota GOTO,¹⁾ Ren FUCHIZAWA¹⁾ and Ken HIGUCHI¹⁾

¹⁾Muroran Institute of Technology, Muroran, Japan

(Received July 31st, 2015)

We investigate the effects of covering pressure and friction between convex tapes on the bending stiffness and natural frequency of a braid-coated biconvex tape (BCON) boom. We establish an analytical model by comparing experimental and analytical results of BCON booms because the braid-coated boundary conditions of the boom are complicated and the analytical model is difficult to construct. BCON booms will have various uses for regular and large-scale deployable space structures such as solar sails, solar array panels, and de-orbit mechanisms. Thus, the bending stiffness, natural frequency, and structural characteristics after deployment are experimentally measured. Several parametric analyses are also calculated by using the proposed contact analysis model. On the basis of these results, we discuss the effect of the braid coating and future work.

Key Words: Braid-coated Biconvex Tape Boom (BCON Boom), Contact Analysis, Bending Stiffness and Natural Frequency Measurement

1. Introduction

Lightweight deployable booms with a high packing rate and high bending and torsional stiffness are required in space development. Deployable booms are used as actuators during deployment and as structural members after deployment in lightweight, large-scale space structures such as gossamer structures. However, these properties are contradictory and it is difficult to create booms that satisfy every property. Thus, trade-offs and design optimizations are considered in developing many types of deployable booms.

Various types of booms have been developed. Inflatable booms are the lightest and have the highest packing rate,^{1, 2)} although the interior of the boom must be highly pressurized or the outer inflatable tube material must be rigidized¹⁻⁶⁾ to achieve and maintain high bending and torsional stiffness after deployment. A storable tubular extendable member (STEM) boom^{7, 8)} consisting of tri-axial woven fabric and carbon fiber-reinforced plastic can maintain high stiffness after deployment. However, uni-STEM booms^{7, 8)} have a low torsional stiffness due to their open cross-section, whereas a bi-STEM boom is twice the weight of a uni-STEM boom. Round-section^{9, 10)} or double-omega-section¹¹⁻¹³⁾ booms have high bending and torsional stiffness. However, the packing rate is low because these booms cannot slide in the boom's lengthwise direction during packing owing to the tight boundary edge between the semicircular or omega sections. The unslidable packing means that the packed configuration has gaps in the roll.

The braid-coated biconvex tape (BCON) boom^{14, 15)} design, which combines double convex tapes forming an elliptical cross section and slidable boundary conditions due to the braid coating, will be optimized (Fig. 1). In addition, it can deploy itself by releasing the elastic energy stored during packing. From a structural point of view, the BCON boom has many advantages. However, quantitative parametric studies on the curvature of the convex tapes, friction between convex tapes,

covering pressures of the braid, and the relationship between the covering pressures and bending and torsional stiffness, have yet to be performed. The curvature of convex tapes directly and geometrically affects the bending and torsional stiffness, although the curvature of convex tapes is higher because the semicircular cross section is difficult to maintain because of unstable edge contacts. The friction between the convex tape and the covering pressure affect the sliding behavior in the lengthwise direction during and after deployment and the bending stiffness or deformation. The low friction allows easy, smooth deployment, but the easy sliding decreases the bending stiffness. High friction or tight covering create high bending stiffness; however, these conditions impede sliding and may jam the boom during deployment. To adapt to various mission requirements, the effect of these parameters and the optimum values should be obtained quantitatively.

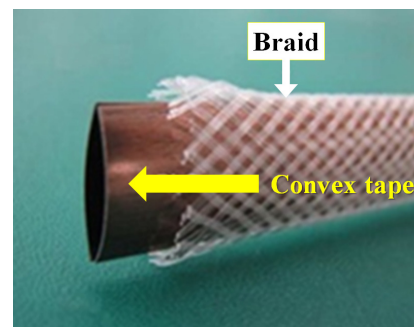


Fig. 1. Photograph of the BCON boom.

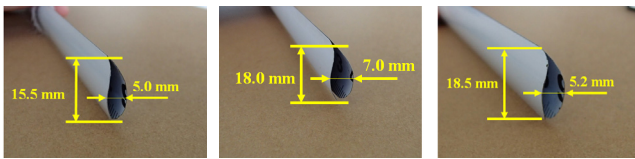
In this work, we perform experimental and analytical studies to measure the relationship between the covering pressure and structural stiffness and to establish analytical models of the BCON boom. The bending stiffness is measured experimentally for three BCON booms with different cross sections, and the natural frequency in the bending direction is measured by the free vibration method. The covering pressure

of the BCON boom is parametrically controlled by changing the tension of the braid for each measurement. In the analytical approaches, the bending stiffness and the natural frequency are calculated by using commercially available software, ANSYS. The effects of the braid coating are modeled as the covering pressure acting around the outside of the analytical convex tape model. The friction and the contact between convex tapes are also included in these analyses. On the basis of the experimental and analytical results, the effects of the covering pressure and friction of the BCON boom on the structural characteristics are discussed.

2. Experimental Bending Displacement and Natural Frequency Measurements

2.1. Test pieces and test equipment

To investigate the effects of the curvature of convex tape and covering pressure on the bending and natural frequency of BCON booms, three laboratory-scale test pieces are handcrafted (Types A–C). Commercial tape springs are used for convex tapes and the convex tape material is carbon steel or carbon tool steel. The length of each test piece is 540 mm. To eliminate variation due to individual differences, three different test pieces (Nos. 1–3) are prepared for each type of cross section. Fig. 2 shows the cross sections of the test pieces and Table 1 shows their parameters.



(a) Type A. (b) Type B. (c) Type C.
Fig. 2. Cross-sectional shapes of test pieces.

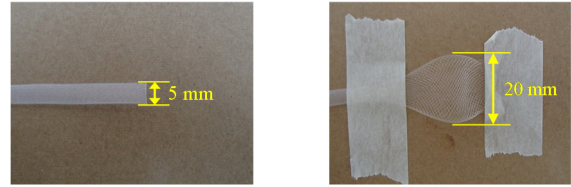
Table 1. Test piece parameters.

Test piece type	Material	Length [mm]	Thickness [mm]	Width [mm]	Distance between biconvex sides [mm]	Radius of curvature [mm]
A	Carbon tool steel	500	0.20	15.50	5.00	14.04
B	Carbon steel			18.00	7.50	13.77
C	Carbon tool steel			18.50	5.20	18.85

The braid fibers are made from PFA and have a diameter of 0.15 mm. Sixty-four fibers are used for braiding, the width of the unstretched braid is 5 mm (Fig. 3 (a)), and that of the stretched braid is a maximum of about 20 mm (Fig. 3 (b)).

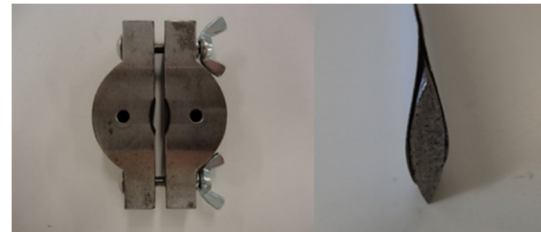
To maintain the cross section of the BCON boom test pieces during measurements, fixing tools were designed (Fig. 4). Fixing tools consist of outer and inner tools. The curvatures of the outer and inner tools are the same as those of the convex tapes. The outer tool holds the braid tightly, maintaining the covering pressure and braid tension around the test pieces. The braid tension is measured by using a spring scale. The braid is

directly connected to the spring scale, and one edge is held tightly with the fixing tools and the other edge is free. After applying tension to the braid, the free edge is also held tightly (Fig. 5). The tension applied to the braid is 0.5 and 1.0 kgf (1.0 kgf = 9.8 N).



(a) Unstretched. (b) Stretched.

Fig. 3. Braid for covering convex tapes.



(a) Outer tool (b) Inner tool

Fig. 4. Fixing tools for measurement.



Fig. 5. Control method for braid tension.

2.2. Bending displacement measurement

The experimental apparatus for the bending test is shown in Fig. 6. One edge is fixed with a support device, and the other edge is hung from the spring scale, with the free edge in the bending direction. Before adding bending loads, a preload is added to cancel gravitational force. After applying a 0.01 kgf load to the free edge side, the displacement of the free end is measured. For each type of test piece (Types A–C) three different pieces (Nos. 1–3) were measured five times, making a total of 15 measurements for each type of test piece. The braid tension value is 0.5 and 1.0 kgf. The results of the measurements are shown in Table 2.

The bending displacement at a braid tension of 1.0 kgf is larger than that at 0.5 kgf for every test piece except for Type A, No. 1. This means that the bending stiffness decreases because of the increased compressive force on the convex tapes resulting from the braid tension. The tensed braid configuration behaves like a tensed spring and the compressive force acts between the tightly fixed edges. Both compressive force and bending force act in these measurements and the higher compression of the convex tapes results in larger bending displacement. However, the friction force between convex tapes also affects the bending stiffness, and the higher covering pressure increases the friction. The combined effects of the compressive force and friction are measured in this experiment, and the specific measurement of each effect is planned in future work.

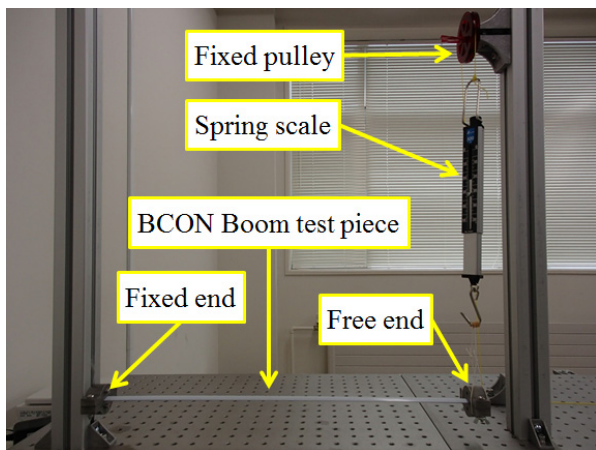


Fig. 6. Experimental apparatus for the bending test.

Table 2. Bending test results.

(a) Type A

Test piece	No. 1		No. 2		No. 3		
	0.5 kgf	1.0 kgf	0.5 kgf	1.0 kgf	0.5 kgf	1.0 kgf	
Displacement [mm]	1st	2.45	2.58	2.42	2.70	2.58	2.92
	2nd	2.42	2.40	2.59	2.69	2.42	2.96
	3rd	2.55	2.36	2.46	2.97	2.44	2.81
	4th	2.50	2.44	2.52	2.88	2.46	2.95
	5th	2.45	2.19	2.60	2.89	2.45	2.80
Average	2.47	2.39	2.52	2.83	2.47	2.89	
Overall average [mm]	0.5 kgf		1.0 kgf		1.0 kgf		

(b) Type B

Test piece	No. 1		No. 2		No. 3		
	0.5 kgf	1.0 kgf	0.5 kgf	1.0 kgf	0.5 kgf	1.0 kgf	
Displacement [mm]	1st	0.63	0.84	0.60	0.86	0.57	0.81
	2nd	0.77	0.96	0.43	0.89	0.49	0.94
	3rd	0.39	0.85	0.45	0.85	0.57	0.88
	4th	0.53	0.91	0.70	0.92	0.63	0.91
	5th	0.57	0.77	0.62	0.96	0.53	0.83
Average	0.58	0.87	0.56	0.90	0.56	0.87	
Overall average [mm]	0.5 kgf		1.0 kgf		1.0 kgf		

(c) Type C

Test piece	No. 1		No. 2		No. 3		
	0.5 kgf	1.0 kgf	0.5 kgf	1.0 kgf	0.5 kgf	1.0 kgf	
Displacement [mm]	1st	0.67	0.94	0.71	1.15	0.67	1.05
	2nd	0.66	1.11	0.64	1.05	0.77	1.14
	3rd	0.72	1.02	0.66	1.09	0.70	1.20
	4th	0.74	1.13	0.64	1.05	0.76	1.13
	5th	0.65	1.02	0.74	0.96	0.72	1.02
Average	0.69	1.04	0.68	1.06	0.72	1.11	
Overall average [mm]	0.5 kgf		1.0 kgf		1.0 kgf		

2.3. Natural frequency measurement

The natural frequency in the bending direction is measured by using the free vibration method. Figure 7 shows a test piece before it is placed in the experimental apparatus and Fig. 8 shows the vibration test apparatus. In this measurement, one edge is held by the fixing tool and the other free end side is held by the heat sealed braid to eliminate the effect of the fixing tool mass during vibration. The length of the test pieces is 520 mm. To eliminate the effect of gravity force, test pieces are set vertically on a support device. The initial displacement of the test piece tip is 5 mm, and the displacement of test piece tip during free vibration behavior is measured by using a laser displacement meter. Similar to the former bending displacement measurements, three different pieces of the three types of test pieces are measured. The braid covering pressure is the same as before, and two braid tensions are used.

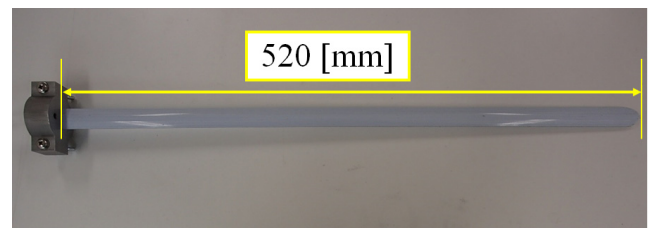


Fig. 7. Test piece for vibration test.

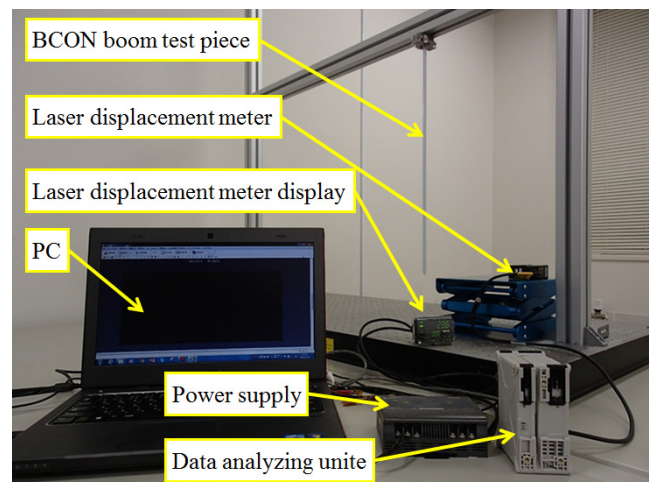


Fig. 8. Experimental apparatus for vibration test.

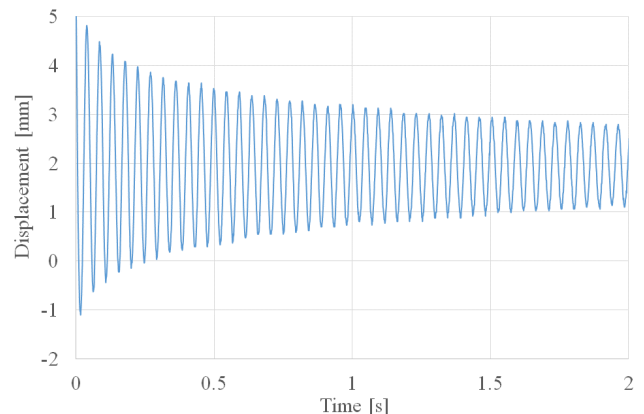


Fig. 9. Example of vibration wave.

Figure 9 shows an example of a measured vibration waveform. The first mode natural frequency toward the bending direction is obtained by applying FFT analysis to the vibration waves. Table 3 shows the first mode natural frequency of each test piece.

For types B and C, the natural frequency value for the 1.0 kgf braid tension force is 0.5% to 1.0% higher than for the 0.5 kgf force. For type A, the natural frequency values are the same for braid tension forces of 0.5 and 1.0 kgf. The same natural frequencies are measured under the different braid tension conditions. The combined effects of the compressive force and the friction affect the vibration behavior, canceling each other out, so that similar natural frequencies are obtained. Therefore, the compressive force decreases the natural frequency and friction increases it. In future work, we plan to measure the effects of the compressive force and friction force on the dynamic behavior of the BCON boom separately.

Table 3. First mode natural frequencies.

(a) Type A

Test piece		No. 1		No. 2		No. 3	
Braid tension		0.5 kgf	1.0 kgf	0.5 kgf	1.0 kgf	0.5 kgf	1.0 kgf
Natural frequency [Hz]	1st	15.38	15.38	15.38	15.38	15.38	15.38
	2nd	15.38	15.38	15.38	15.38	15.38	15.38
	3rd	15.38	15.38	15.38	15.38	15.38	15.38
	4th	15.38	15.38	15.38	15.38	15.38	15.38
	5th	15.38	15.38	15.38	15.38	15.38	15.38
Average		15.38	15.38	15.38	15.38	15.38	15.38
Overall average [Hz]		0.5 kgf		1.0 kgf		15.38	15.38

(b) Type B

Test piece		No. 1		No. 2		No. 3	
Braid tension		0.5 kgf	1.0 kgf	0.5 kgf	1.0 kgf	0.5 kgf	1.0 kgf
Natural frequency [Hz]	1st	21.97	21.97	21.97	22.22	22.22	21.97
	2nd	21.97	21.97	21.97	22.22	22.22	21.97
	3rd	21.97	21.97	21.97	22.22	22.22	21.97
	4th	21.73	21.97	21.97	22.22	22.22	21.97
	5th	21.73	21.97	21.97	22.22	22.22	21.97
Average		21.87	21.97	21.97	22.22	22.22	21.97
Overall average [Hz]		0.5 kgf		1.0 kgf		22.02	22.05

(c) Type C

Test piece		No. 1		No. 2		No. 3	
Braid tension		0.5 kgf	1.0 kgf	0.5 kgf	1.0 kgf	0.5 kgf	1.0 kgf
Natural frequency [Hz]	1st	18.80	18.80	18.80	19.04	18.55	19.04
	2nd	18.80	18.80	18.80	19.04	18.55	19.04
	3rd	18.80	18.80	18.80	19.04	18.55	19.04
	4th	18.80	18.80	18.80	19.04	18.55	19.04
	5th	18.80	18.80	18.80	19.04	18.55	19.04
Average		18.80	18.80	18.80	19.04	18.55	19.04
Overall average [Hz]		0.5 kgf		1.0 kgf		18.72	18.96

3. Analytical Modeling of Bending Displacement and Natural Frequency

3.1. Proposed analytical model of BCON boom

Before considering the proposed model, an analytical model consisting of biconvex tape connected by springs was examined. The braid coating was modeled as springs, and the springs were located between the convex tape line edges at 5 mm intervals in a lengthwise direction. The merits of this model are simplicity and low calculation costs. However, the restoring forces of the spring act in only the displacement mode where the convex tape is displaced in a different direction. When the convex tape is displaced in the same direction, the effect of the spring is lost and the effect of the braid coating is not modeled. Based on this initial model, a contact analysis model where covering pressure is applied to the outer surface of the convex tape is developed. In this model, the surface-to-surface and line edge-to-surface contact is considered (Figs. 10 and 11). These two types of contact definitions prevent penetration among the convex tapes during analysis and keep the calculations stable. As shown as Fig. 12, the braid coating is modeled as pressure acting on the outer surface of the model. In addition, the friction between the convex tapes is also an important factor in the structural characteristics and its effect can be considered by using contact analysis. The friction effect is defined all over the convex tapes, although the friction force mainly acts in the line edge of the convex tapes (yellow lines, Fig. 11).

The geometrical parameters and material constants of the model are shown in Fig. 13 and Table 4. These parameters are suitable for the Type A test piece in the experiments. Eight node shell elements are used in this model. The thickness of the analytical model is changed by 0.1 mm because the paint

thickness of commercially available convex tapes is neglected. To obtain stable calculation conditions, the following boundary conditions are set for the calculations: Y direction displacement and rotation around the Z-axis for every node on X = 0 are fixed. The same Y direction displacement is possible between the right and left convex tape line edges (yellow lines, Fig. 11). The effect of the compressive force in the lengthwise direction of the convex tapes is also important, as discussed in the experimental section; however, it is not considered in this analysis because of the unstable calculation results. An extra boundary condition or another model will be required for compressive force effect analysis, which we intend to examine in future work.

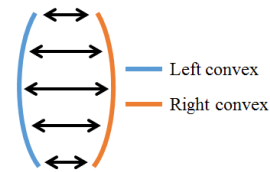


Fig. 10. Surface-to-surface contact definition.

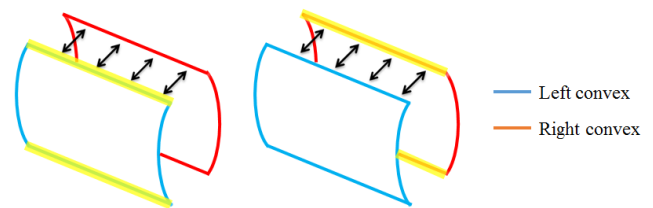


Fig. 11. Line edge-to-surface contact definition.

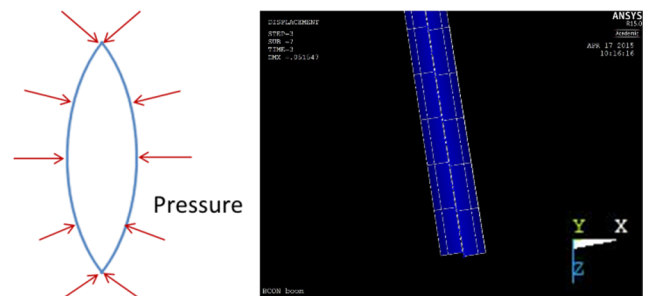


Fig. 12. Covering pressure definition and friction between convex tapes.

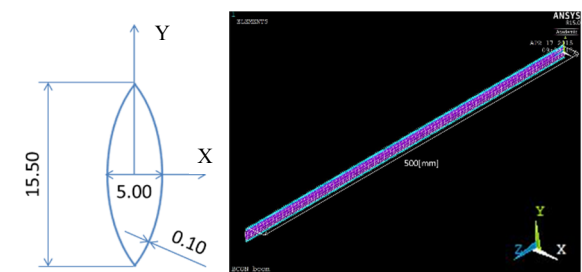


Fig. 13. Analysis model of the BCON boom.

Table 4. Material constants of carbon tool steels.

Material		Carbon tool steels
Young's modulus	GPa	208
Poisson's ratio		0.30
Density	g/cm ³	7.689

3.2. Bending displacement analysis while changing covering pressure and friction coefficient

Bending displacements for various covering pressures and friction conditions are analyzed to understand their effect on bending behavior. In Fig. 14, the X- and Y-axes are in the cross section surface of the analytical model, and the Z-axis is in the lengthwise direction. The fixed end of the analytical model at the origin ($Z = 0$), and the concentrated load of 0.01 kgf is applied to the opposite free end tip (white arrow, Fig. 14), as in the experimental analysis. To maintain the cross section shape of the free end edge, the Y direction displacement and Z-axis rotation on each node in the free end tips are zero.

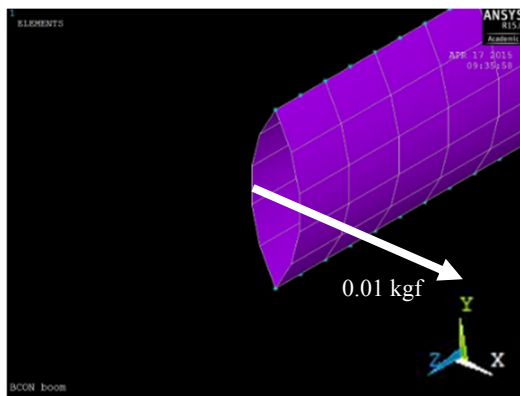


Fig. 14. Load conditions.

Figure 15 shows the relationship between the covering pressure and the bending displacement. The effect of the covering pressure is similar from 1 to 100 Pa for all friction coefficients, and its effects are shown after 100 Pa. The effective value of the covering pressure depends strongly on the friction coefficient.

Figure 16 shows the relationship between the friction coefficient and the bending displacement. As in Fig. 15, the effect of the friction and friction coefficient is only shown for a covering pressure of more than 100 Pa. Comparing the results at covering pressures between 5000 and 10,000 Pa for a friction coefficient from 0 to 0.2, the effect of friction is greater than that of the covering pressure in static BCON boom bending displacement because the amount of bending displacement decreases dramatically at a friction coefficient of 0 to 0.2. However, that value is almost same for covering pressures of 5000 and 10,000 Pa. Furthermore, a similar bending displacement is obtained for friction coefficients from 0.2 to 1 at covering pressures of 5000 and 10,000 Pa. Comparing these analytical results with the experimental results (Table 2 (a)), the actual covering pressure value acting on the BCON boom will be more than 100 Pa, and the friction coefficient value will be more than 0.2. Additional parametric analytical results will allow discussion that is more precise and the consideration of the combined effects of covering pressure and friction.

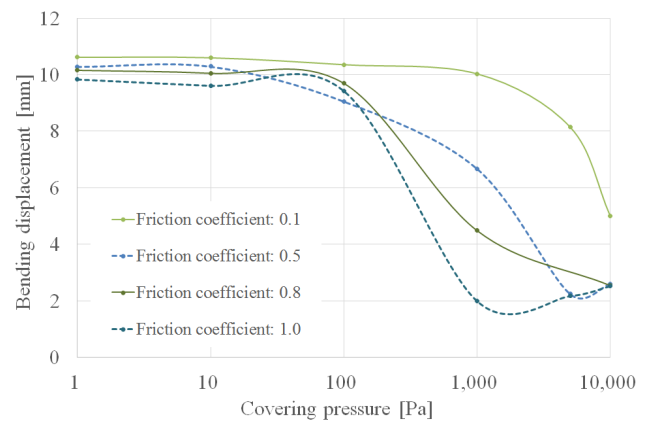


Fig. 15. Bending displacements as a function of covering pressure at various friction coefficients.

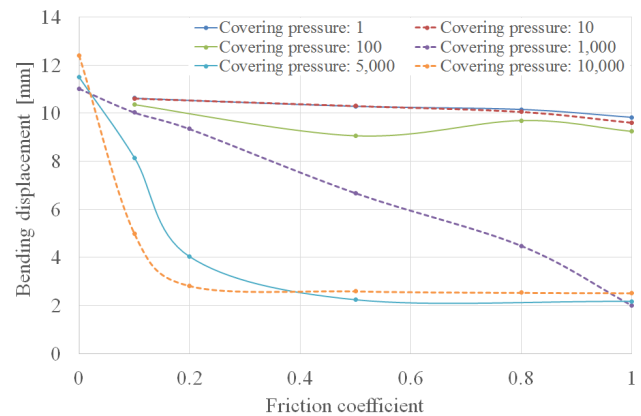


Fig. 16. Bending displacement as a function of friction coefficient at various covering pressures.

3.3. Natural frequency analysis while changing covering pressure and friction coefficient

Similar to the bending displacement analysis, the first-mode natural frequency in the bending direction is analyzed by using the same analytical model, covering pressures, and friction coefficients. The boundary condition for both boom tips is also the same as for the bending displacement analysis. The length of the model is changed to 520 mm to match the experiment conditions. The initial settings are as follows: 5 mm displacement at point 1 in Fig. 17, which is then released and free vibration is allowed. The natural frequency is calculated by the response waveform averaged at point 1 and 2 displacements.

Figure 18 shows the response waveforms for different covering pressures. The friction coefficient is fixed as 0.1 in these analyses. Sliding in the lengthwise direction during the vibration causes friction between the convex tapes, damping the response waveforms. When the covering pressure is more than 100 Pa, the response waveform is damped dramatically. The amplitude of the response waveform also changes drastically just after vibration, and the position of the vibration center changes, as shown in the experimental results in Fig. 9. This vibration behavior is also observed for bi-STEM booms, although the effect of friction on the BCON boom will be larger

because of the covering pressure.

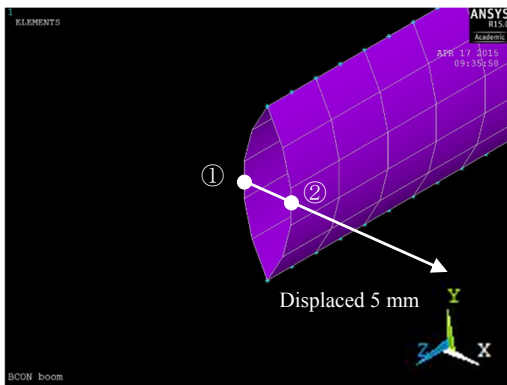


Fig. 17. Initial setting for the natural frequency analysis.

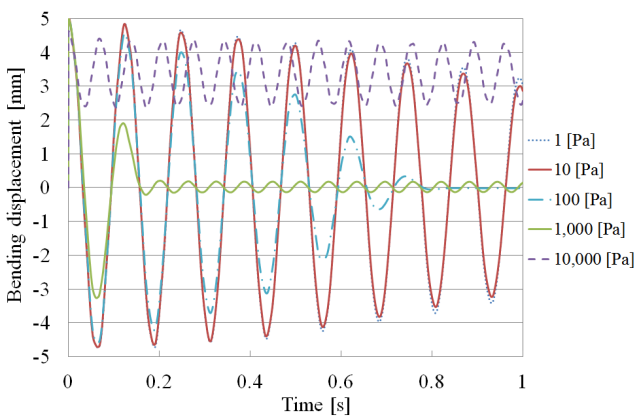


Fig. 18. Response waveform comparison for various covering pressures at a friction coefficient of 0.1.

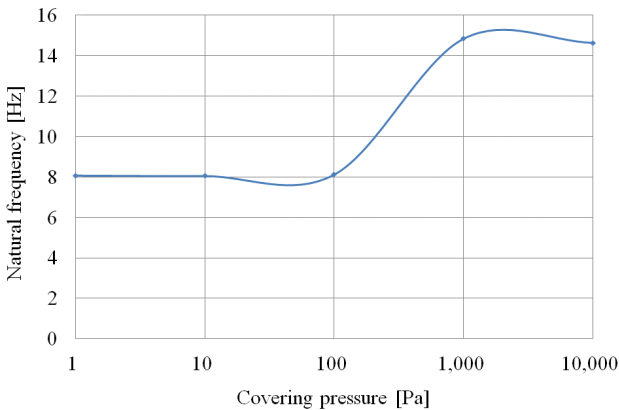


Fig. 19. Natural frequency analysis as a function of covering pressure at a friction coefficient of 0.1.

Fig. 19 shows the natural frequency as a function of covering pressure. The same natural frequency as for the bending displacement analytical results is obtained at covering pressures from 1 to 100 Pa, and the frequency is higher above 100 Pa. This is because each convex tape model vibrates independently at less than 100 Pa, and contact between each convex tape model occurs at more than 100 Pa. The effect of friction works well on the integrated biconvex tape conditions, and the biconvex tape configuration with higher bending stiffness

shows a higher natural frequency for the BCON boom dynamic vibration behavior.

Figure 20 shows the response waveform and Fig. 21 shows the natural frequency as a function of the friction coefficient at a covering pressure of 1000 Pa. The effect of friction damping is larger than in the previous analytical results. The effect of the friction coefficient on the natural frequency is larger than that of the covering pressure because the natural frequency calculation results from 8 to 18.5 Hz for various friction coefficients show a larger range difference than those for various covering pressures from 8 to 15 Hz.

Based on the bending displacement and natural frequency analysis, the proposed contact analysis model can be used to investigate the structural characteristics of BCON booms.

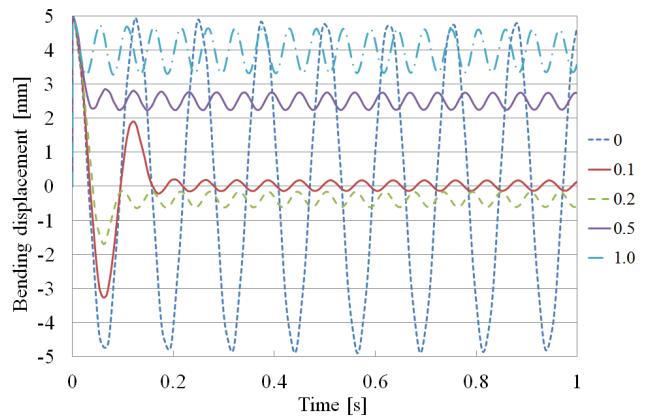


Fig. 20. Response waveform comparison for various friction coefficients at a covering pressure of 1000 Pa.

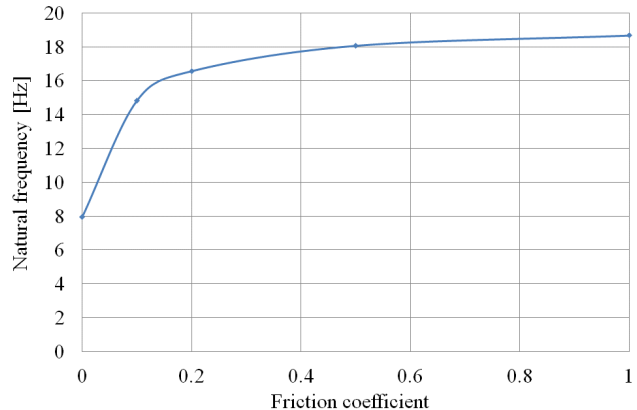


Fig. 21. Natural frequency as a function of friction coefficient at a covering pressure of 1000 Pa.

4. Discussion of Braid Coating

Figure 22 (a) shows a partially magnified photograph of the braid coating and Fig. 22 (b) shows a schematic of the braid coating. The angle of the mesh (yellow line angle, Fig. 22 (a)) is increased by stretching the braid (Fig. 3 (b)), and the angle of the mesh or the space length of the fiber (blue line distance, Fig. 22 (a)) is fixed after inserting a biconvex tape boom and fitting a braid around the convex tape surface by applying tension to

the braid. When the circumference of the biconvex tape ellipse is fixed and the number of fibers in the braid is fixed, the angle of the mesh and the space length of fiber are also fixed (Fig. 22 (b)). When the fit covering condition of the braid is obtained and the extra tension acts on the braid in the lengthwise direction, the covering pressures around the convex tapes and the compressive forces for the convex tapes in the lengthwise direction also increase. In the numerical analysis, increasing the covering pressures also increases the friction force. The increased friction force causes the high bending stiffness and natural frequency. However, the increased compressive force degrades these structural characteristics in the experiments. Compressive forces in the lengthwise direction or high friction forces interrupt the deployment of this boom by impeding the sliding of the convex tapes. A trade-off design or adjusting the braid tension will be important in controlling the structural characteristics of BCON booms.

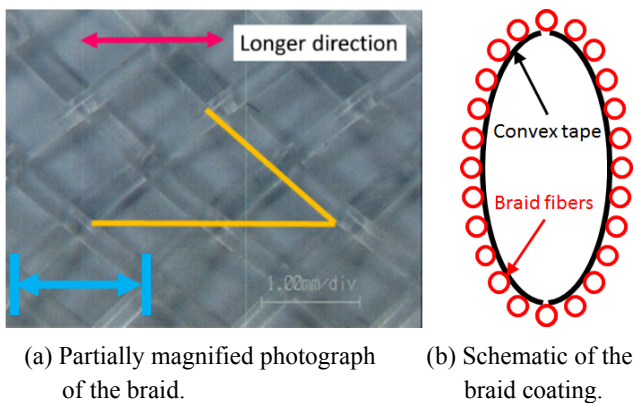


Fig. 22. Braid covering configuration.

5. Conclusion

Experimental and analytical studies of BCON booms focusing on the relationships of covering pressure with bending stiffness and natural frequency were performed. The bending stiffness and the natural frequency were measured experimentally by using three BCON boom models with different cross sections. The combined effect of the compressive force in the lengthwise direction of the boom from the braid tension and the friction force from the covering pressure were considered. These results show that the covering mechanism of braid is not simple, and optimized tension control is important to control the bending stiffness and the natural frequency. We intend to measure the separate effects of the compressive force and friction force from the braid tension in future work. We also proposed a contact analysis model, in which the bending stiffness and natural frequency were calculated by parametrically changing the covering pressure and the friction coefficient. The effects of the covering pressure and friction coefficient on the bending displacement and the natural frequency were analyzed.

Next, we intend to establish an engineering model of the braid coating to calculate the actual covering pressure and

friction coefficient of the booms, and to compare the experimental and analytical results. In addition, the analytical model should also include the effect of compressive force and identify the individual effects of the covering pressure, friction, and compressive force.

Acknowledgments

The authors thank Ryoji Sakai, Akihito Watanabe and Toshiyuki Hori, SAKASE ADTECH CO., LTD. for providing the braid used in this research.

References

- 1) Lichodziejewski D., Derbès B., Slade K. and Mann T.: Vacuum Deployment and Testing of a 4-Quadrant Scalable Inflatable Rigidizable Solar Sail System, *46th AIAA/ASME/ASCE/AHS/ASC Structures, Structural Dynamics & Materials (SDM) Conf.*, Austin, Texas, 2005, AIAA 2005-2122.
- 2) Lichodziejewski D., Gordon V. and Derbès, B.: Spiral Wrapped Aluminum Laminate Rigidization Technology, *43rd AIAA / ASME / ASCE / AHS / ASC Structures, Structural Dynamics, and Materials Conf.*, Denver, Colorado, 2002, AIAA 2002-1701.
- 3) M. Lou, H. Fang and L-M. Hsia: Self-Rigidizable Space Inflatable Tube, *J. Spacecraft and Rockets*, **39**, No.5 (2002), pp.682-690.
- 4) Watanabe, A. Hori, T. and Tsunoda, H.: Fiber and Fabric Technologies for Space Inflatable Structures, *Proc. 47th United Conf. Space Science and Technology (Ukaren)*, 2G1 (2003), pp. 958-963 (in Japanese).
- 5) Watanabe, A., Sakai, R., Hori, T. and Ito, H.: Study on Light Curable Space Inflatable Structures Technology by Triaxial Woven Fabric, *Proc. 50th United Conf. Space Science and Technology (Ukaren)*, 3E05 (2006), pp. 1693-1698 (in Japanese).
- 6) Watanabe, A. Hori, T. and Sakai, R.: Study of Space Inflatable Structures by Chain Curing Polymer, *Proc. 53th United Conf. Space Science and Technology (Ukaren)*, 2H11 (2009), pp. 1509-1512 (in Japanese).
- 7) Iqbal, K. and Pellegrino, S.: Bi-Stable Composite Shells, *41st AIAA / ASME / ASCE / AHS / ASC Structures, Structural Dynamics, and Materials Conf.*, Atlanta, GA, 2000, AIAA 2000-1385.
- 8) Craig, S. H., Keith, R. G., Erik, R. A., Robert, J. D. and Mark, S. L.: Development of a Prototype Elastic Memory Composite STEM for Large Space Structures, *44th AIAA / ASME / ASCE / AHS / ASC Structures, Structural Dynamics, and Materials Conf.*, Norfolk, VA, 2003, AIAA 2003-1977.
- 9) Sakamoto, H., Furuya, H., Sato, Y., Natori, M.C. et al.: Origami-Based Membrane Storage and Deployment Technology for De-Orbiting Satellites, *64th International Astronautical Congress*, Beijing, China, 2013, IAC-13-B4.6A.4.
- 10) Ömer, S.: Deployment analysis of a self-deployable composite boom, *Composite Structures*, **89** (2009), pp. 374–381.
- 11) Herbeck, L., Strcöhlein, T. and Torrez-Torres, J.: Lightweight Deployable Booms: Design, Manufacture, Verification, and Smart Materials Application, *55th International Astronautical Congress, IAF/IAA/IISL*, Vancouver, Canada, 2004, IAC-04-I.4.10.
- 12) Christoph, S., Lars, H. and Elmar, B.: Structural engineering on deployable CFRP booms for a solar propelled sailcraft, *Acta Astronautica*, **58** (2006), pp. 185 – 196.
- 13) Joachim, B., Marco, S. and Martin, W.: Ultralight Deployable Booms for Solar Sails and Other Large Gossamer Structures in Space, *Acta Astronautica*, **68** (2011), pp. 984–992
- 14) Watanabe, A. et al.: Study of the extensible structure which coated a braid, *Proc. 56th United Conf. Space Science and Technology (Ukaren)*, 2012, JSASS-2012-4496 (in Japanese).
- 15) Watanabe, A et al., Lightweighting examination of the braid coated boom, *Proc. 57th United Conf. Space Science and Technology (Ukaren)*, 2013, JSASS-2013-4679 (in Japanese).